

PAPER • OPEN ACCESS

The Evaluation of Air Blowing Method of Variable-Air-Conditioning-System using Coanda Effect by Computational Fluid Dynamics

To cite this article: H Sakakibara *et al* 2019 *IOP Conf. Ser.: Earth Environ. Sci.* **294** 012058

View the [article online](#) for updates and enhancements.

The Evaluation of Air Blowing Method of Variable-Air-Conditioning-System using Coanda Effect by Computational Fluid Dynamics

H Sakakibara¹, T Akimoto², H Igarashi³, S Nakamura⁴, and M Kimura¹

¹ Graduate Student, Shibaura Institute of Technology, Tokyo, Japan

² Prof., Dept. of Arch., Shibaura Institute of Technology, Tokyo, Japan

³ Shinryo Corporation, Tokyo, Japan

⁴ Mitsubishi Jisho Sekkei Inc., Tokyo, Japan

E-mail: me18047@shibaura-it.ac.jp

Abstract. Government of Japan aims to achieve net zero energy buildings on average regarding newly constructed buildings by 2030. Therefore, we studied the ductless air conditioning system using Coanda effect which is one of the technologies to realize net zero energy buildings. By reducing duct space on the ceiling, it can reduce fan power and save resources. However, when the amount of blowing air volume is small, there is the possibility the conditioned air is not diffuse into the room. Also, when the blowing air volume is large, the draft airflow possibly occurs. Hence, the distribution of the airflow in the room was confirmed by computational fluid dynamics. 15 cases were analysed at the thermal load of 30%, 50% and 100%. The default case was set as the blowing temperature difference of 10 Kelvin and the blowing wind speed of 3.0 meters per second. Then, Air Diffusion Performance Index was calculated from Effective Draft Temperature. As a result, the thermal comfort was generally good when the thermal load was 100%. However, there were some cases that the thermal comfort was low by the draft and hot spaces. It was comfortable in most cases when the thermal load was 30% and 50%.

1. Introduction

In Japan, the Cabinet decided the fifth Strategic Energy Plan in 2018. There, the goal of realizing net zero energy buildings (ZEB) for typical new construction by 2030 is set [1]. As part of this goal, this study focuses on the variable-air-conditioning-system using Coanda effect which is a ductless air conditioning system [2]. The variable-air-conditioning system using Coanda effect is shown in Figure 1. The Coanda effect represents the characteristic of the air flowing along the ceiling surface. The air outlets are arranged so as to blow the conditioned air from the wall position near the ceiling. By reducing duct space on the ceiling, it can reduce fan power and save resources. This air conditioning system attracts attention as one of the approaches to spread ZEB.

The cross-section view of the air outlet is shown in Figure 2. The amount of the air blown out changes depending on the control on the variation of the thermal load in the room. Then, the position where the blown air current peels off from the ceiling surface changes. And there is a risk of problems such as the draft airflow and the conditioned air is not diffuse into the room [3]. In order to solve these problems, there is the mechanism that the air velocity can be autonomously controlled constantly even at the time of varying air volume at the air outlet.



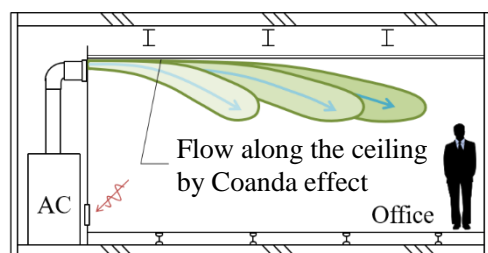


Figure 1. Overview of the variable-air-conditioning system using the Coanda effect

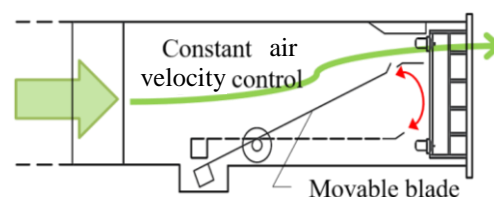


Figure 2. Cross-section view of the air outlet

In this study, we evaluate the air blowing method of the variable-air-conditioning-system using the Coanda effect with computational fluid dynamics (CFD) analysis. The Evaluation was performed at 50% and 30% at low thermal load, in addition to 100% at peak thermal load. The target building is an environmentally-friendly-office building scheduled to be completed in 2020. The architectural overview is shown in table 1.

Table 1. Architectural overview

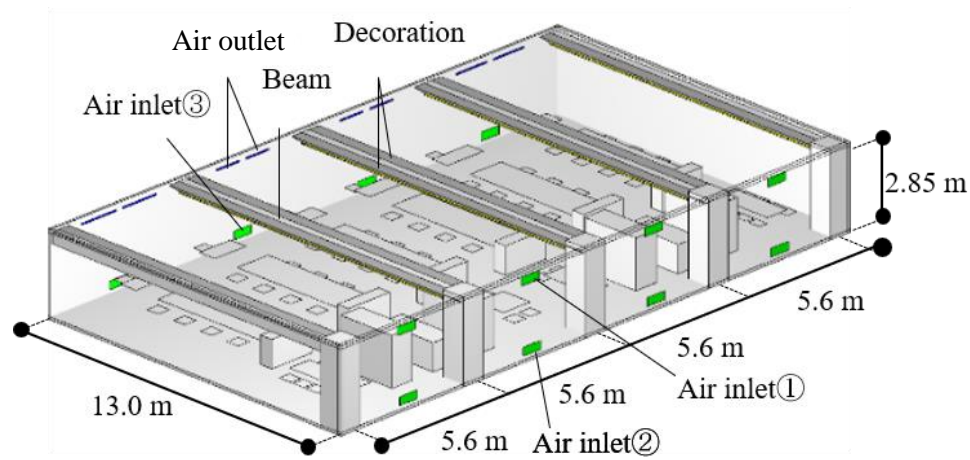
Location	Chiyoda, Tokyo, Japan
Principal Use	Office
Site Area	595 m ²
Construction Area	506 m ²
Total Floor Area	4,656 m ²
Construction	Steel Construction, Steel-Reinforced Concrete
Story	10 (B1F ~ 9F)
Floor Height	3.45 m
Ceiling Height	2.8 m
Commencement	2018
Completion	2020

2. Analysis methods

2.1. Analysis model

The analysis model is shown in Figure3. The model was created using the CFD tool STREAM V12. On the target floor, there are two air outlets with the large aspect ratio per span, on the upper side of one side of the wall. There are air inlets at the top (①) and the bottom (②) on the opposite wall. It is also at the lower part of the wall on the same side as the air outlets (③).

The analysis setting values are shown in Table 2. We reproduced one floor of the target building at 12 o'clock in Tokyo in summer. The thermal load setting values are shown in Table 3. The thermal load was given the indoor load from the lighting, the human, and the office automation equipment in addition to the structure load.

**Figure 3.** Analysis model**Table 2.** Analysis settings

Location	Tokyo, Japan
Season	12 O'clock in Summer
Room Temperature	26 °C
Air Outlet Width	1,500 mm
Air Outlet Height	14 ~ 79 mm

Table 3. Thermal load settings

Thermal Load	30%	50%	100%
Structure Load [W]	878	1,464	2,927
Lightning Load [W]	761	1,268	2,536
Human Load [W]	1,274	2,124	4,247
Equipment Load [W]	2,378	3,963	7,925

2.2. Mesh division

The width of the mesh was about 100 mm. The width of the first mesh from the wall surface was made 10 to 20 mm. The Size ratio of the adjacent mesh was set at maximum 2. The aspect ratio of the mesh is set to 10 at the maximum. Mesh division was done in detail, especially around air outlets and the wall surface.

Conditions were calculated using the standard $k - \epsilon$ turbulence model. The SIMPLEC method was adopted for analysis. The QUICK scheme was used as the difference scheme of the advection term of the equation of motion.

2.3. Analysis cases

Analysis cases are shown in Table 4. 15 cases were analyzed at 30%, 50% and 100% thermal load rate. For the default case (Case 1), the air velocity was set to 3 m / s and the outlet temperature difference was set to 8 °C. The suction rate was 50% at each air inlet ③ and ① on the opposite wall.

2.4. Evaluation method

The thermal comfort was evaluated by air diffusion performance index (ADPI) and the throw length. ADPI is the volume ratio of the comfort zone of effective draft temperature (EDT) (1) in the residential area (floor + 0 to 1.7 m). The throw length was defined as the average distance from each air outlet to the position where the air velocity near the ceiling was 0.25 m / s or less.

$$EDT = (t_x - t_c) - 8 (V_x - 0.15) \quad (1)$$

t_x : Local Temperature

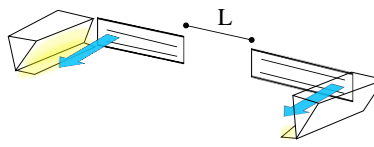
t_c : Average Temperature

V_x : Local Air Velocity

Comfort zone: $V_x \leq 0.35$ [m/s] and $-1.7 \leq EDT \leq 1.1$ [°C]

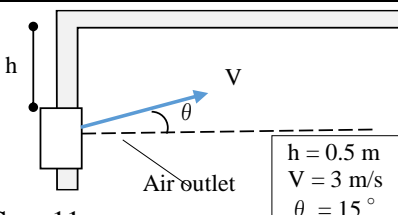
Table 4. Parameters of the analysed cases

Case		Air Velocity [m / s]	Temperature Difference [°C]	Air Volume [m ³ / h]			Outlet Interval [m]	Outlet Position [m]	Suction Ratio [%]				
				Thermal Load									
				30%	50%	100%							
1	Default Case	3.0	8	499	831	1,663	0.3	CH – 0.1	①50 ③50				
2	High Air Velocity	4.0											
3	Small Temperature Difference	3.0	6	665	1,108	2,217							
4	Large Temperature Difference		10	399	665	1,330							
5	Large Outlet Distance		8	499	831	1,663	0.9						
6	Adjacent to Beam						2.0						
7	Adjacent to Beam (No Decoration)						2.0						
8	Suction from ①						0.3		①100				
9	Suction from ②								②100				
10	Suction from ③								③100				
11	Elevation Angle 15 °						8	499	831	1,663	0.3	CH – 0.5	①50 ③50
12	Elevation Angles 15 °and -15 °											CH – 0.1	
13	Range Angle 30 °												
14	Ceiling Louver												
15	Diffusion Wing												



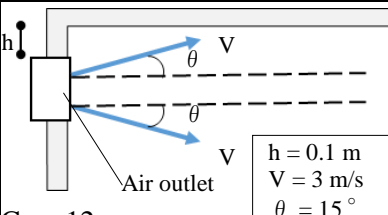
Case 6

$L = 2 \text{ m}$



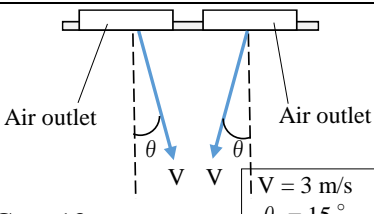
Case 11

$h = 0.5 \text{ m}$
 $V = 3 \text{ m/s}$
 $\theta = 15^\circ$



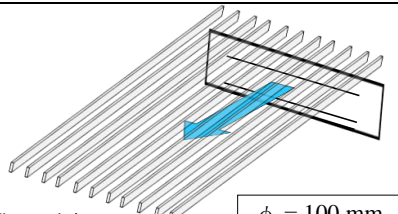
Case 12

$h = 0.1 \text{ m}$
 $V = 3 \text{ m/s}$
 $\theta = 15^\circ$



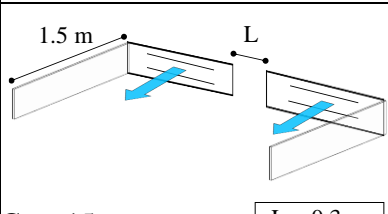
Case 13

$V = 3 \text{ m/s}$
 $\theta = 15^\circ$



Case 14

$\phi = 100 \text{ mm}$



Case 15

$L = 0.3 \text{ m}$

3. Analysis results

The throw length and the calculated ADPI for all cases are shown in table 5.

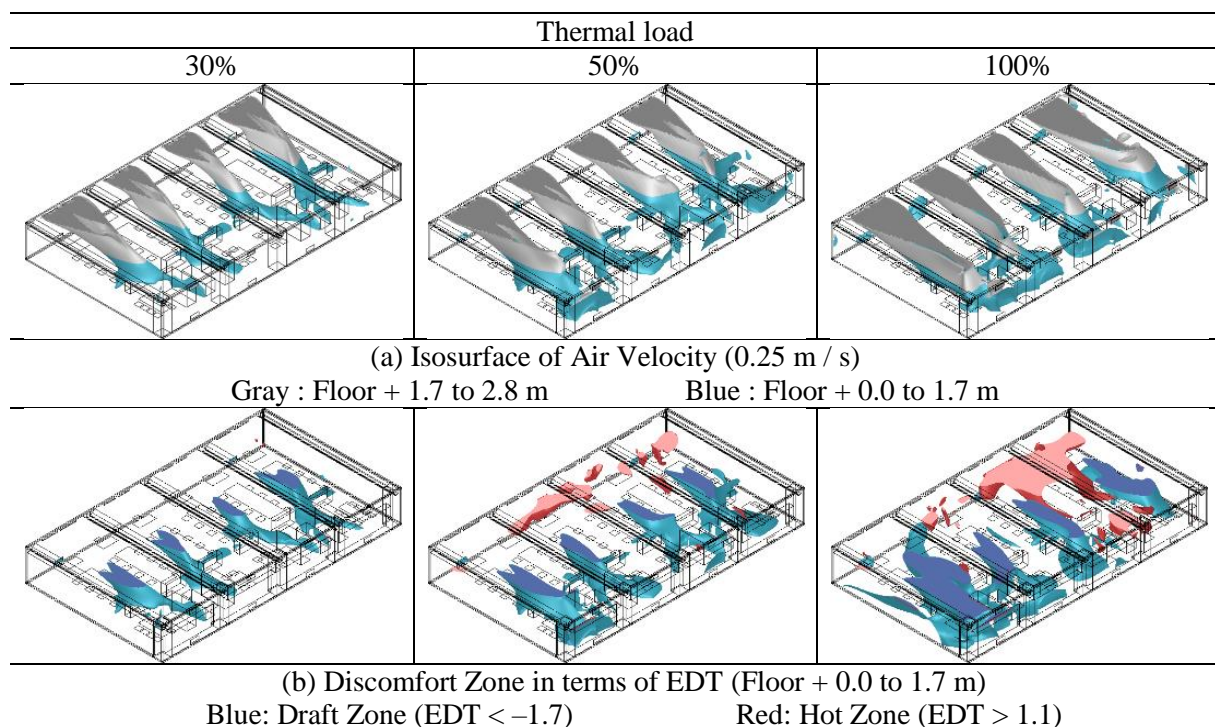
Table 5. Throw lengths and ADPI (Relative values compared to the default case are color-coded)

Case	Throw length [m]			ADPI [%]		
	Thermal Load			Thermal Load		
	30%	50%	100%	30%	50%	100%
Case 1	4.8	7.4	9.2	97	93	85
Case 2	6.5	8.9	12.0	97	95	84
Case 3	7.4	9.2	12.5	96	93	84
Case 4	4.0	5.7	7.8	96	92	83
Case 5	4.4	6.5	7.5	97	95	86
Case 6	5.4	6.3	9.5	99	97	87
Case 7	5.1	8.1	10.5	98	95	84
Case 8	5.1	7.0	8.7	96	93	86
Case 9	5.2	7.1	9.3	97	93	81
Case 10	5.2	7.3	8.7	97	94	83
Case 11	5.0	7.3	8.4	98	94	79
Case 12	4.5	5.8	8.9	95	90	72
Case 13	3.9	4.9	5.8	94	90	77
Case 14	8.1	12.0	12.9	95	80	74
Case 15	4.6	7.3	9.5	97	94	87

Min. Case 1 Max.

In Case 1 (see Table 6), ADPI exceeded 90% at 30% and 50% thermal load. Even at 100% thermal load, ADPI exceeded 80% and was generally comfortable.

Table 6. Analysis results of Case 1

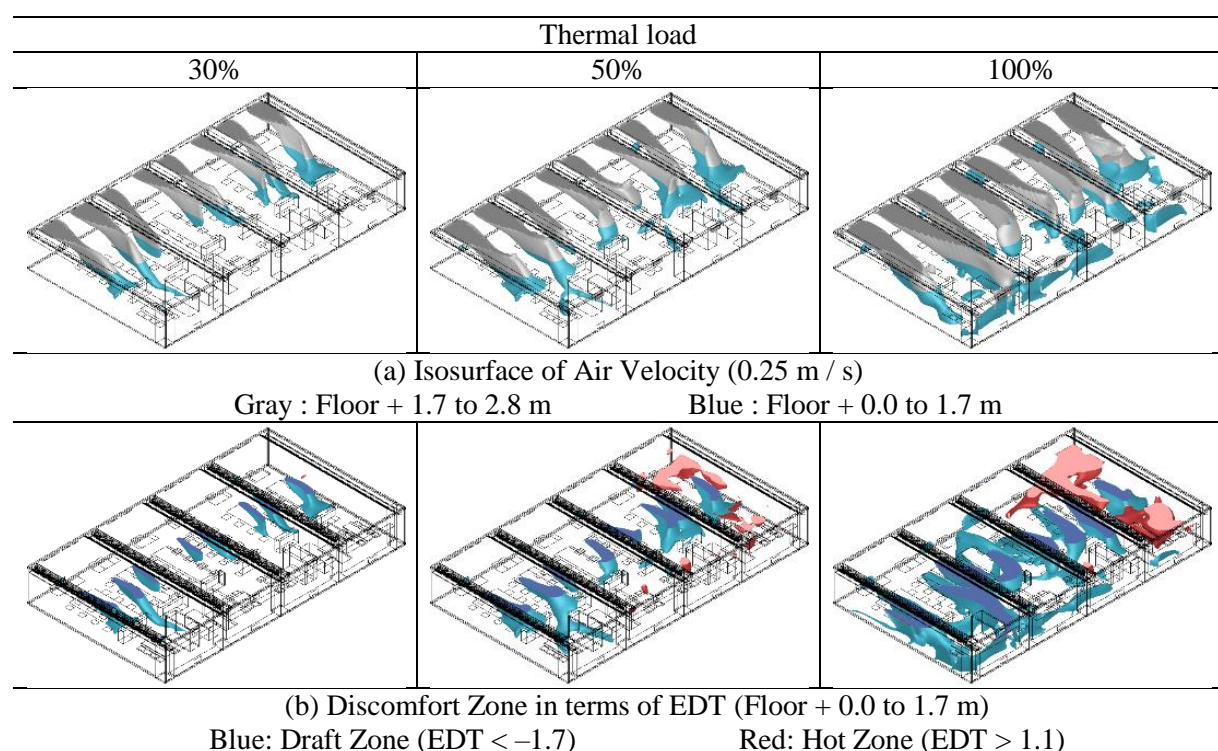


In Case 2, the throw length increased in all thermal loads compared to Case 1. However, almost no change was seen in ADPI.

In Case 3, the throw length increased in all thermal loads compared to Case 1. However, ADPI decreased in all thermal loads. In Case 4, the throw length shrank in all thermal loads compared to Case 1. ADPI also decreased in all thermal loads.

In Case 5, the throw length increased in all thermal loads compared to Case 1. However, ADPI increased in all thermal loads. In Case 6 (see Table 7), the throw length shrank at 50% thermal load compared to Case 1. The throw length increased at 30% and 100% thermal load. However, ADPI increased in all thermal loads regardless of the distance increase or decrease. In Case 7, the throw length increased in all thermal loads compared to Case 1. However, almost no change was seen in ADPI.

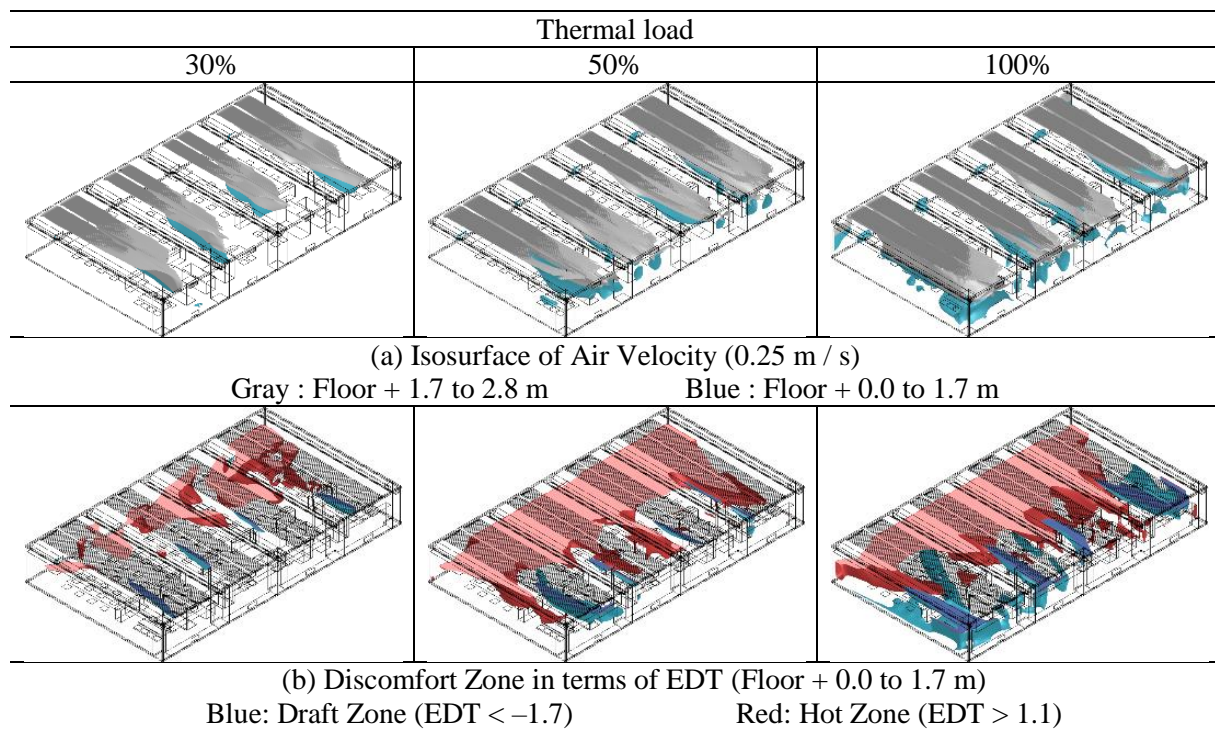
Table 7. Analysis results of Case 6



In Case 8, there was not much change in the throw length at all thermal loads compared to Case 1. Similarly, ADPI showed almost no change. In Cases 9 and 10, there was not much change in throw length at all thermal loads compared to Case 1. ADPI was slightly decreased at 100% thermal load.

In case 11, the throw length shrank at 100% thermal load compared to Case 1. ADPI also decreased at 100% thermal load. In Cases 12 and 13, the distance shrank significantly in all thermal loads compared to case 1. ADPI also decreased significantly in all thermal loads.

In Case 14 (see Table 8), the throw length increased drastically in all thermal loads compared to Case 1. However, ADPI decreased significantly in all thermal loads.

Table 8. Analysis results of Case 14

In Case 15, there was not much change in the throw length at all thermal loads compared to Case 1. However, ADPI increased at 30% and 100% thermal load.

4. Discussions and conclusion

In Case 2, the throw length exceeded Case 1 at all thermal load rates. Therefore, we think that throw length tends to increase as air velocity increases.

From cases 1, 3, and 4, the smaller the temperature difference of the blowing air is, the more the throw length tends to be extended. However, when the temperature difference of the blowing air is small, the air volume increases. Also, when the temperature difference of the blowing air is increased, the risk of the draft airflow also rises.

For Cases 5, 6, ADPI exceeds Case 1 at all thermal load rates. This observation shows that expansion of the spacing between adjacent outlets reduces the heat pool and draft airflow and improves perceived comfort. Furthermore, in Case 7, by blowing out adjacent to the beam, the beam prevents air from drawing in, so the airflow is stabilized and the projection length is increased.

Cases 8, 9 and 10 show that the influence of the suction position on the throw length is not effective.

In Cases 11, 12, and 13, the throw length and ADPI at 100% thermal load are both lower than in Case 1. It seems that the blowing angle is not appropriate for the airflow.

In Case 14, the throw length exceeded Case 1 at all thermal load rates. However, hot pool occurred in the space on the air conditioner side, and ADPI fell below 80% when the thermal load was 100%.

In Case 15, the throw length decreased when the thermal load was 50% or less. On the other hand, ADPI improved at all thermal load rates. This is understood to be the result of reduced interference of adjacent blowing air and improved diffusivity.

In summary, the indoor thermal environment was comfortable when the thermal load was 50% or less. As the throw length increases, the draft airflow decreases. However, overall perceived comfort can decrease simultaneously due to the generation of hot pool. Also, when the air outlet interval and the diffusion of the airflow in the horizontal direction are increased, the amount of draft airflow is reduced and the thermal comfort is considered to be improved.

References

- [1] Agency for Natural Resources and Energy 2014 *Strategic Energy Plan* 38
- [2] Akimoto T, Hatori D, Hirasuga N, Kato S, Ueda T and Sakamoto Y 2017 Plan and verification of a midsize office aiming for zeb (part 1) energy-saving building facility technologies on a midsize office *Technical Papers of SHASE* **10** 345-8
- [3] Igarashi H, Akimoto T, Hatori D, Hirasuga N, Chiba A, Takasu H, Ohata S, Ueda T, Sakamoto Y and Yamakita S 2017 Plan and verification of a midsize office aiming for zeb (part 5) indoor environment and air flow characteristics of the variable-air-volume air-conditioning system using the coanda effect *Technical Papers of SHASE* **10** 361-4